NON RIGID IMAGE REGISTRATION BY MODELING DEFORMATIONS AS ELASTIC WAVES

Sahar Ahmad and Muhammad Faisal Khan

National University of Sciences and Technology (NUST)
College of Telecommunication Engineering
Islamabad, Pakistan

ABSTRACT

In this paper we propose an inter-subject non-rigid image registration method that is derived from the concept of elastodynamics. Non-rigid warps are modeled as elastic waves which tend to recover extensive deformations. The deformable transformation model is given by Navier PDE which is solved iteratively using finite difference approximations. The dynamical displacements so computed represent the warp field which is then used to bring the subject image into spatial correspondence with the atlas. The results were validated using Jaccard coefficient (J), Dice coefficient (D), Overlap coefficient (O) and Normalized Cross Correlation (NCC) with $mean \pm std$ values of $0.81 \pm .04$, $0.89 \pm .03$, $0.99 \pm .01$ and $0.97 \pm .01$ respectively. This quantitative assessment confirmed that the proposed registration method performs very well.

Index Terms— Elastodynamics, Image Registration, Magnetic Resonance Imaging (MRI), Medical Image Analysis

1. INTRODUCTION

Medical imaging technology has revolutionized medical and clinical practices. It emerged as a tool for the visualization and inspection of anatomical structures [1] but today it is extensively used for surgical planning and navigation [2], dosage planning [3] and for monitoring syndrome development [4]. Medical image analysis [5] aids scientists and clinicians in neuroscience for computational anatomy, volumetric analysis and brain development studies. Non-rigid image registration is a key enabling technique that is used for medical image analysis and image guided surgery [6] as it helps neurosurgeons in accurate localization of anatomical structures. It facilitates in gaining knowledge about the location of anatomical structures, tissue type, structural boundaries etc. by registering the subject image onto an atlas where the structures have superior visibility. This constitute a class of registration known as inter-subject registration.

This paper presents a new physical model based inter-subject non-rigid image registration algorithm that is inspired by the theory of elastodynamics. The image under deformation is modeled as an elastic material over which waves are generated due to the action of unbalanced external force. These time varying elastic waves demonstrate the local warps within the image and enable the modeling of large extensive deformations. The non-rigid transformation is determined by computing the dynamic displacement field described by elastodynamics wave equation. The inertial forces carry out the registration process and towards the end, the elastic material is brought into equilibrium state i.e. the waves die out as the two images become similar to each other.

Current research on non-rigid transformation model divides them into two broad categories:
Parametric models: These models are derived from interpolation and approximation theory which includes radial basis functions (e.g. Thin plate splines [7], multiquadrics [8], weighted mean [9], Wendland $\psi-$ Functions [10] etc.).
Non parametric models: These are derived from physical models based on the notion of continuum mechanics (e.g. linear elastic model [11], viscous fluid flow model [12], diffusion model [13]) and curvature registration [14].
The existing linear elastic model is based on the notion of elastostatics which assumes that under the action of applied force, the elastic body undergoes static deformations i.e. small displacements. Hence it can only recover small deformations. On the other hand, viscous fluid flow model based on fluid's physical properties models the motion of voxels over time as velocity field. It can recover large deformations but it is computationally inefficient due to time integration of the velocity field in order to get the displacement field.

2. THEORY OF ELASTODYNAMICS

The underlying idea of elastodynamics is that when the equilibrium of elastic body is disturbed, it is set into motion. This motion depicts waves characteristics because every point in the body is not disturbed simultaneously rather this disturbance propagates over time [15]. Thus elastodynamics relies on the study of elastic waves, constituting the subject of time varying linear elastic theory.

Consider an elastic medium that undergoes dynamical displacement ζ under the action of an unbalanced force $\mathbf{f}$ known as inertial force, produced by stress $\mathbf{S}$.

$$\mathbf{f} = -\nabla.\mathbf{S} = \mu\nabla^2\zeta + (\mu+\lambda)\,\nabla.\nabla\zeta \tag{1}$$

According to law of conservation of momentum, the inertial force must produce a rate of change of momentum given by the Navier partial differential equation [16];

$$\mu\nabla^2\zeta + (\mu+\lambda)\,\nabla.\nabla\zeta = -\nabla.\mathbf{S} = \rho\frac{\partial^2\zeta}{\partial t^2} \tag{2}$$

Eq (2) is only for homogeneous and isotropic media where ρ is the material density, μ is the shear modulus and λ is the Lame's coefficient. The wave equation of elastodynamics is similar to elastostatic equilibrium equation except for the additional acceleration term. The elastostatic equation is given by Navier-Cauchy partial differential equation as;

$$\mu\nabla^2\zeta + (\mu+\lambda)\,\nabla.\nabla\zeta = -\nabla.\mathbf{S} \tag{3}$$

The elastic deformations require the position of particle to be represented in Lagrangian reference frame where the reference point moves with the particle. Eulerian reference frame is required to represent the particle's position for fluid deformation where the point of reference is fixed. Since the wave equation is linear it has same Eulerian and Lagrangian representations, difference occurs only when there are non linear terms.

3. MATERIALS

The T1 weighted MR images of human head for 12 subjects were acquired using Philips Medical Systems Gyroscan 1.5T MRI scanner. One 2D axial slice from each subject were selected at visibly same location in superior-inferior axis. These slices had 256x256 pixels with in-plane resolution of $1mm$. The atlas image was acquired using 3D Turbo Flash 3T MRI scanner. Similar 2D axial slice of atlas was extracted which had resolution of 256x256 with pixel size of $1mm^2$. The skull was segmented from all the images using morphological operations.

4. METHODS

In this paper we present an inter-subject non-rigid registration framework based on elastodynamics wave equation. We propose to model the image as an elastic solid that under the influence of external force undergoes dynamical deformations such that the perturbations characterize wave-like behaviour. Thus the registration problem is formulated as solving the hyperbolic wave equation and finding the displacement vector $\mathbf{u}$ which maps every pixel $\mathbf{x}= [x_x\ x_y]^T$ in the source image $J(\mathbf{x})$ to corresponding pixel in the reference image $I(\mathbf{x})$.

Let $\mathbf{u} = [u_x\ u_y]^T$ be the displacement vector. The wave equation as transformation function for each coordinate direction is expressed as;

$$\mu\nabla^2 u_x + (\mu+\lambda)\,\nabla.\nabla u_x + f_x = \rho\frac{\partial^2 u_x}{\partial t^2} \tag{4}$$

$$\mu\nabla^2 u_y + (\mu+\lambda)\,\nabla.\nabla u_y + f_y = \rho\frac{\partial^2 u_y}{\partial t^2}, \tag{5}$$

where μ, λ and ρ control the amount of deformations. If their value is too large then the image depicts a rigid material and it becomes hard to deform. In contrast, if the value of these constants is too small then the image represents an extremely flexible material such that the system becomes unstable. f_x and f_y are the inertial forces for horizontal and vertical components respectively described as follows;

$$f_x = -k_1\left(J\left(\mathbf{x}+\mathbf{u}\right) - I\left(\mathbf{x}\right)\right)\frac{\partial J\left(\mathbf{x}+\mathbf{u}\right)}{\partial(x_x+u_x)} \tag{6}$$

$$f_y = -k_2\left(J\left(\mathbf{x}+\mathbf{u}\right) - I\left(\mathbf{x}\right)\right)\frac{\partial J\left(\mathbf{x}+\mathbf{u}\right)}{\partial(x_y+u_y)}, \tag{7}$$

where k_1 and k_2 are the constants.

4.1. Proposed Algorithm

The proposed algorithm for non-rigid registration of MR images has following steps:

1. Initially the current and the previous displacement vectors or the warp fields are set to zero (the rest state) i.e. $u_x(\mathbf{x};t_0) = u_x(\mathbf{x};t_1) = 0$ and $u_y(\mathbf{x};t_0) = u_y(\mathbf{x};t_1) = 0$.

2. The whole registration process is driven by the inertial forces. The quantity within brackets in eq (6) and eq (7) gives the difference between the two images and the derivative term gives the direction of change in the deformed image. The constants k_1 and k_2 are iteratively increased with the constant step size. If the mean value of the inertial force falls below the threshold then the warp field is not updated otherwise proceed to step 3. The threshold value is experimentally set to 10^{-5}.

3. Solve the partial differential equation given by eq (4) and eq (5). Finite difference approximation is used to compute the warp field, as given by eq (8) and eq (9). The values of the constants are experimentally set as: μ=0.5, λ=0 and ρ=4.

$$u_x(\mathbf{x};t_{n+1}) = \frac{\mu\nabla^2 u_x(\mathbf{x};t_n) + \mu\nabla.\nabla u_x(\mathbf{x};t_n) + f_x}{\rho} + 2u_x(\mathbf{x};t_n) - u_x(\mathbf{x};t_{n-1}) \tag{8}$$

$$u_y(\mathbf{x};t_{n+1}) = \frac{\mu\nabla^2 u_y(\mathbf{x};t_n) + \mu\nabla.\nabla u_y(\mathbf{x};t_n) + f_y}{\rho} + 2u_y(\mathbf{x};t_n) - u_y(\mathbf{x};t_{n-1}) \tag{9}$$

4. The warp field so computed is now used to deform the source image. The transformed pixel coordinates $\mathbf{X}=[X_x\ X_y]^T$ are then given as:

$$X_x = x_x + u_x \tag{10}$$

$$X_y = x_y + u_y \tag{11}$$

4.2. Validation

The qualitative and quantitative analysis of registration accuracy was conducted by performing the proposed 2D non-rigid image registration on 12 subject MR brain images. The results were qualitatively evaluated using the checkerboard display of the atlas image and the registered subject images. This visualization tool overlays the two images and the degree of alignment is checked at the structural boundaries. For visual analysis, atlas and the subject images (both pre-registered and post-registered) were also fused. Apart from qualitative analysis, the quantitaive evaluation was carried out by area overlap measurement. For this purpose the lateral ventricles (left and right) were manually delineated from the atlas image and the subject images since it has well defined boundaries. Let S_1 be the lateral ventricular region segmented from atlas image and S_2 be the lateral ventricular region segmented from a subject image and transformed into the atlas domain after non-rigid image registration. Jaccard coefficient J [17], Dice coefficient D [18] and Overlap coefficient O [19] were calculated as follows;

$$J = \frac{|S_1 \cap S_2|}{|S_1 \cup S_2|} \tag{12}$$

$$D = \frac{2\,|S_1 \cap S_2|}{|S_1| + |S_2|} \tag{13}$$

$$O = \frac{|S_1 \cap S_2|}{min\,[|S_1|\ , |S_2|]} \tag{14}$$

Besides the overlap measurement tools, normalized cross correlation (NCC) [20] was also used to quantify the degree of accuracy of registration result. NCC was computed over the whole image domain.

5. RESULTS AND DISCUSSION

The 2D axial MR slice of the atlas (Fig. 1(a)) and the subject (Fig. 1(b)) were used for the registration procedure. It can be seen in Fig. 1 that skull is segmented and only brain region is used for the registration. The transformation for each coordinate direction was determined using the discretized version of elastodynamics wave equation given by eq 8 and eq 9. The resulting warp field was used to iteratively deform the subject image so that it gets aligned with the atlas. Checkerboard display of the axial view of the atlas and the pre-registered subject image is shown in Fig. 2(a). It can be observed that the two images are clearly misaligned. The corresponding

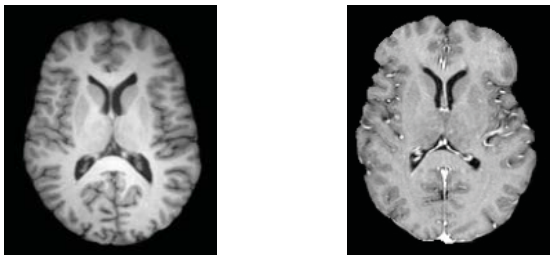

(a) (b)

Fig. 1. 2D axial MR slice of (a) the atlas image and (b) the subject image.

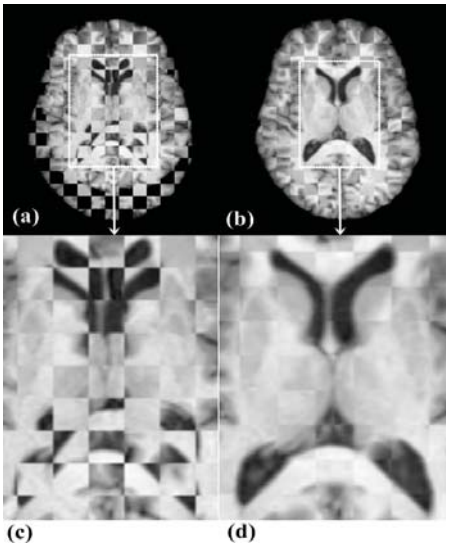

Fig. 2. Checkerboard display of the atlas and one of the subject image (a) before registration and (b) after registration procedure (b). The corresponding zoomed-in ventricular region is shown in (c) and (d). Note the well aligned ventricles in (d).

zoomed-in view of the ventricular region is shown in Fig. 2(c). Fig. 2(b) shows the result of the proposed registration process. The zoomed view of the ventricular region is shown in Fig. 2(d). One can see in Fig. 2 that our registration procedure resulted in a very good alignment of ventricles. Image fusion was also used as a visualization tool to assess the quality of registration. Fig. 3(a) shows the fusion of atlas and 12 pre-registered subject images. It can be observed that the fused images are blurred with no overlapping structures whereas in Fig. 3(b) the fusion of atlas and 12 post-registered subjects resulted in a smooth display.

The quantitative evaluation of the registration accuracy was carried out by manually segmenting the lateral ventricles from the atlas and subject images. These segmentation maps were then used for overlap measurement using J, D and O. Besides this NCC was also used to evaluate registration ac-

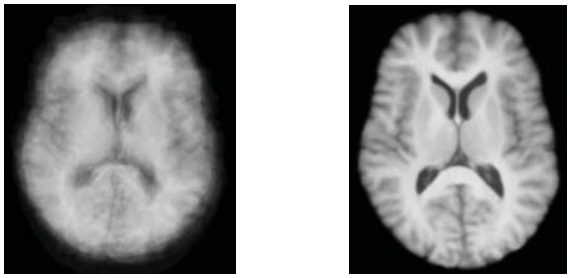

(a) (b)

Fig. 3. Image fusion of axial slice of atlas and (a) 12 pre-registered subject images and (b) with 12 post-registered subject images. Note the blurred fusion in (a) and smooth fusion in (b).

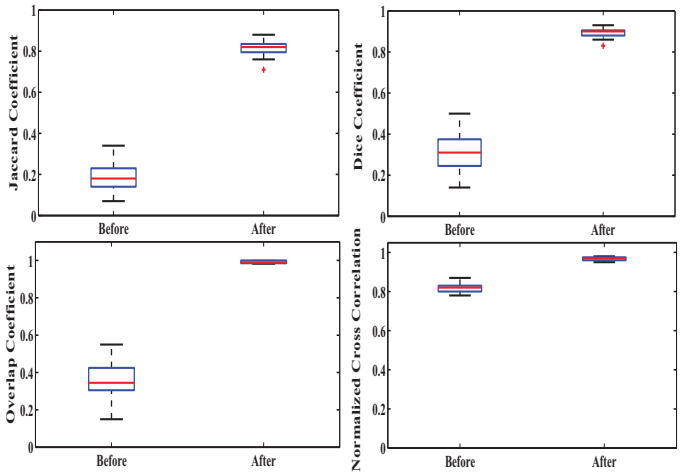

Fig. 4. Accuracy comparison of the proposed registration procedure in terms of (a) Jaccard Coefficient, (b) Dice Coefficient, (c) Overlap Coefficient and (d) Normalized Cross Correlation.

curacy. The statistical evaluation of J, D, O and NCC is given in Table 1 which shows the $mean \pm std$ for all the 12 subjects. The $mean \pm std$ of J is $0.81 \pm .04$, D is $0.89 \pm .03$, O is $0.99 \pm .01$ and NCC is $0.97 \pm .01$ over ventricles. Boxplots of the assesment tools before and after image registration is shown in Fig. 4. These boxplots indicate that before registration data was widely distributed and had lower values whereas after non rigid registration the spread of the data became narrower and had higher values close to one. This proved that our proposed method yielded high quality registration results.

6. CONCLUSION

This paper presented a non-rigid image registration scheme based on the concept of elastodynamics. The non-rigid deformations are modeled as elastic waves which are generated due to dynamical perturbations in an elastic medium under the action of inertial force. The proposed elastic wave model is able to recover large deformations well. The qualitative and quantitative assessment of the results signify that our proposed registration method achieves very good alignment.

Table 1. Statistical Evaluation of J, D, O and NCC for Segmented Lateral Ventricles in 12 Different Subjects

Subjects	J	D	O	NCC
1	0.82	0.90	0.99	0.96
2	0.88	0.93	0.98	0.97
3	0.76	0.86	1.0	0.96
4	0.85	0.92	0.98	0.96
5	0.81	0.89	0.99	0.95
6	0.83	0.90	0.99	0.97
7	0.82	0.90	0.99	0.98
8	0.71	0.83	1.0	0.97
9	0.78	0.87	1.0	0.96
10	0.82	0.90	1.0	0.98
11	0.84	0.91	0.98	0.97
12	0.81	0.89	0.99	0.98
$mean$ $\pm std$	0.81 $\pm .04$	0.89 $\pm .03$	0.99 $\pm .01$	0.97 $\pm .01$

7. REFERENCES

[1] Q. Wei, Y. Hu, G. Gelfand, and J.H. MacGregor, "Segmentation of lung lobes in high resolution isotropic CT images," *IEEE Transactions on Biomedical Engineering*, vol. 56, pp. 1383–1393, May 2009.

[2] T. Kuo, T. Wong, T. Wu, and J. Fang, "Optical tracking-based model surgery for orthognathic surgical planning using a quantifying evaluation method," *IEEE Transactions on Information Technology in Biomedicine*, vol. 16, pp. 1193–1199, November 2012.

[3] C. Lu, S. Chelikani, D.A. Jaffray, M.F. Milosevic, L.H. Staib, and J.S. Duncan, "Simultaneous non-rigid registration, segmentation and tumor detection in MRI guided cervical cancer radiation therapy," *IEEE Transactions on Medical Imaging*, vol. 31, pp. 1213–1227, June 2012.

[4] S. Bauer, C. May, D. Dionysiou, G. Stamatakos, P. Buchler, and M. Reyes, "Multiscale modeling for image analysis of brain tumor studies," *IEEE Transactions on Biomedical Engineering*, vol. 59, pp. 25–29, January 2012.

[5] S.D. Olabarriaga, J.G. Snel, C.P. Botha, and R.G. Belleman, "Integrated support for medical image analy-

sis methods: From development to clinical application," *IEEE Transactions on Information Technology in Biomedicine*, vol. 11, pp. 47–57, January 2006.

[6] R.E. Ong, C. Glisson, H. Altamar, D. Viprakasit, P. Clark, S.D. Herrell, and R.L. Galloway, "Intraprocedural registration for image-guided kidney surgery," *IEEE/ASME Transactions on Mechatronics*, vol. 15, pp. 847–852, December 2010.

[7] F.L. Bookstein, "Principal warps: Thin plate splines and the decomposition of deformations," *IEEE transactions on Pattern Analysis and Machine Intelligence*, vol. 11, pp. 567–585, June 1989.

[8] M.D. Buhmann, "Radial basis functions," *Acta Numerica*, vol. 9, pp. 1–38, 2000.

[9] L. Zagorchev and A. Goshtasby, "A comparative study of transformation functions for nonrigid image registration," *IEEE Transactions on Image Processing*, vol. 15, pp. 529–538, March 2006.

[10] M. Fornefett, K. Rohr, and H.S. Steihl, "Radial basis functions with compact support for elastic registration of medical images," *Image Visualization and Computing*, vol. 19, pp. 87–96, 2001.

[11] C. Broit, *Optimal registration of deformed images*, Ph.D. thesis, University of Pennsylvania, Philadelphia, 1981.

[12] G.E. Christensen, R.D. Rabbitt, and M.I. Miller, "Deformable templates using large deformation kinematics," *IEEE Transactions on Image Processing*, vol. 5, pp. 1435–1447, October 1996.

[13] J.P. Thirion, "Image matching as a diffusion process: An analogy with Maxwell's demons," *Medical Image Analysis*, vol. 2, pp. 243–260, 1998.

[14] S. Henn, "A full curvature based algorithm for image registration," *Journal of Mathematical Imaging and Vision*, vol. 24, pp. 195–208, 2006.

[15] V.B. Poruchikov, *Methods of the classical theory of elastodynamics*, Springer Berlin Heidelberg, 1993.

[16] P.K. Kythe, *Fundamental solutions for differential operators and applications*, pp. 162–179, Springer, 1996.

[17] P. Jaccard, "The distribution of the flora in the alpine zone," *New Phytologist*, vol. 11, pp. 37–50, 1912.

[18] R.L. Dice, "Measures of the amount of ecologic association between species," *Ecology*, vol. 26, pp. 297–302, 1945.

[19] S. Mizuno, "Overlap coefficient for assessing the similarity of pharmacokinetic data between ethnically different populations," *Clinical trials*, vol. 2, pp. 174–181, 2005.

[20] M. Holden, D.L.G. Hill, E.R.E. Denton, J.M. Jarosz, T.C.S. Cox, T. Rohlfing, J. Goodey, and D.J. Hawkes, "Voxel similarity measures for 3D serial MR brain image registration," *IEEE Transactions on Medical Imaging*, vol. 19, pp. 94–102, February 2000.